

Orbiting phenomena in black hole scattering

D. Batic¹, N. G. Kelkar² and M. Nowakowski²

¹ *Dept. of Mathematics, Univ. of West Indies, Kingston 6, Jamaica*

² *Dept. de Fisica, Universidad de los Andes,
Cra.1E No.18A-10, Bogota, Colombia*

Abstract

Rainbow, glory and orbiting scattering are usually described by the properties of the classical deflection function related to the real part of the quantum mechanical scattering phase shift or by the diffractive pattern of the quantum mechanical cross sections. Here we show that the case of orbiting scattering of massless spin 0, 1 and 2 particles from Schwarzschild black holes can be characterized by a sudden rise in $|R_l|^2$ at a critical angular momentum l_C , which we show corresponds to the unstable circular orbits of these particles. For the cases, $s = 0, 2$, we attempt a new interpretation of the Regge-Wheeler potential by identifying the quantum mechanical corrections to the effective potential of massless particles. We probe into the black hole scattering by using numerical and semi-analytical methods which give very good agreements with the exact numerical results. The limitations of previously used approximations as compared to the exact and semi-analytical results are discussed.

PACS numbers: 04.70.Bw, 04.70.Dy, 03.65.Nk

I. INTRODUCTION

Over the last four decades, the physics of particle scattering from different kinds of black holes was one of the most active topics of strong gravitational fields. Apart from the quasinormal modes which, in principle, can be identified as the poles of the corresponding black hole scattering matrix, the behaviour of the cross section with respect to the scattering angle is one of the most interesting features in this area. The key issues around which the physics of black hole scattering centers are related to phenomena such as glory, orbiting (or spiralling), rainbow and super-radiant scattering. One should note that these features are observed experimentally and studied extensively theoretically in nucleus-nucleus scattering. It is gratifying to see similar phenomena occurring in black hole scattering [1]. In the pioneering papers of Ford and Wheeler [2], using semi-classical arguments, a connection between the classical rainbow, glory and orbiting phenomena was made with their quantum mechanical counterparts. Starting with a procedure as proposed by Mott and Massey [3] which gave the classical cross section $\sigma_{cl} = \sigma_{semicl}$, the authors noticed that the classical deflection function can be written in terms of the quantum mechanical scattering phase shift as $\Theta(l(b)) = 2d[\Re\delta_l]/dl$, where l is the angular momentum and b the impact parameter. For particles scattered into the solid angle $\Omega(\theta, \phi)$, the cross sectional area can be written as, $d\sigma = b db d\phi$, so that the differential cross section is proportional to $|db/d\theta|/\sin(\theta)$. The classical angular momentum is $L = bp$. Going over to the quantum mechanical case, if we now consider the de Broglie wavelength $\lambda = k^{-1}$ of the particle to be small compared to the range of the force, we may write, $b = L/p \simeq \sqrt{l(l+1)}/k$. In fact, while working with semi-classical approximations such as the WKB, one must replace $l(l+1) \rightarrow (l+1/2)^2$. In the article of Ford and Wheeler, the authors thus obtain the differential cross section proportional to $(d\Theta/dl)/\sin(\theta)$, which is divergent when the scattering angle θ is 0 or π . Glory is characterized by $\Theta(l)$ passing with finite slope through $0, \pm\pi$ etc and rainbow by the maxima or minima in $\Theta(l)$. If the deflection function displays a singularity at a certain critical value l_C of l , they show that $\Theta(l)$ will vary logarithmically near $l = l_C$. For values of l below and above l_C the particle would have spiralling trajectories and $l = l_C$ would give the limit of an unstable circular orbit. For a particle incident with energy E and for an effective potential, V_{eff} , which is the sum of an actual interaction potential and a centrifugal term, the condition corresponding to such an orbit was shown to be $V_{eff}(r_C, l_C) = E$ (which as we shall

see later is $V_{eff}(r_C, l_C) = \omega^2$ for massless particles with $E^2 = \omega^2$), where r_C is the position of the maximum of the effective potential and E the available energy. Quantum mechanically, one does not get divergent cross sections. One rather observes peaks in the cross sections as a function of angle in the backward directions for glory and orbiting scattering.

Based on the works of Ford and Wheeler, the characterization of the above phenomena in black hole scattering is mostly done in literature by noting the behaviour of the real part of the scattering phase shift or by looking at the oscillating patterns in the cross sections at backward angles. In the present work, we relate the phenomenon of orbiting scattering to the imaginary part of the scattering phase shift. To be specific we evaluate the reflection coefficient in black hole scattering from Schwarzschild black holes by solving the corresponding Riccati equation numerically. Finding a sudden rise of the reflection coefficient, $|R_l|^2 = \exp(-4\delta_l^I)$ plotted as a function of l , at a certain critical value of l for different energies and different spins ($s = 0, 1, 2$) of the massless scattering particles, we show that this critical l is nothing but the l_C corresponding to the unstable circular orbit. We also find that the normalized $|R_l|^2$ always passes through a value of $1/2$ at the critical value l_C .

The present work differs from others [1] in view of the points mentioned above. The reflection coefficient is evaluated exactly using the variable amplitude method as compared to approximate calculations (third reference in [1]), [4]. We also find a potential proportional to $\cosh^{-2}(\alpha x - \beta)$ which gives remarkably good results when compared with the numerical ones. For this potential the transmission coefficients can be found analytically. Parametrizing the \cosh^{-2} potential to fit the Regge-Wheeler potential, we find semi-analytical results for black hole scattering. Even though the scattering off black holes is a widely explored area, not much attention has been paid to the orbiting phenomenon (mostly the glory and rainbow effects have been discussed). Here we supplement the existing literature by a detailed study of how the existence of a classical orbit gets reflected in the quantum mechanical expressions of the scattering of a massless particle from a black hole. This leads to a conjecture regarding quantum corrections to the classical effective potential for massless particles.

In the next section, we provide briefly the formalism for black hole scattering in general and go on to discuss the critical parameters relevant to orbiting and glory scattering. In section III, we discuss the calculation of the reflection coefficient and present results regarding its connection to orbiting scattering. We also present a conjecture related to these phenom-

ena. In section IV we discuss how the Regge-Wheeler potential can be re-interpreted as an effective potential plus quantum corrections proportional \hbar . In section V we summarize our findings.

II. BLACK HOLE SCATTERING

We start by presenting some generalities in black hole scattering. Consider the propagation of a massless scalar field $\phi = \phi(t, r, \vartheta, \varphi)$ governed by the wave equation $g^{\mu\nu}\nabla_\mu\nabla_\nu\phi = 0$ where $g_{\mu\nu}$ denotes a static, spherically symmetric black hole metric whose line element is

$$ds^2 = f(r)dt^2 - \frac{dr^2}{f(r)} - r^2(d\vartheta^2 + \sin^2\vartheta d\varphi^2).$$

Using the following ansatz

$$\phi(t, r, \vartheta, \varphi) = e^{i\omega t} \frac{1}{r} \psi_{n\ell\omega}(r) Y_{\ell m}(\vartheta, \varphi), \quad \text{Re}(\omega) > 0 \quad (1)$$

it is standard [5] to reduce the above equation to a Schrödinger-like equation for the radial part

$$\left[-\frac{d^2}{dr_*^2} + V(r) \right] \psi_{n\ell\omega} = \omega^2 \psi_{n\ell\omega}, \quad (2)$$

where in principle $\omega \equiv \omega_n$, but we shall drop the subscript for convenience in what follows. Moreover, $V(r) = f(r)U(r)$ (with the form of $f(r)$ depending on the metric under consideration) and

$$U(r) = \frac{l(l+1)}{r^2} + \frac{f'(r)}{r}. \quad (3)$$

Here, a prime denotes differentiation with respect to r whereas r_* is a tortoise coordinate defined through

$$\frac{dr_*}{dr} = f(r)^{-1}.$$

A. Scattering from a Schwarzschild black hole

In case of the Schwarzschild metric which we shall consider in the present work, $f(r) = 1 - 2M/r$ where M is the mass of the black hole and the tortoise coordinate is given by

$$r_* = r + 2M \ln \left(\frac{r}{2M} - 1 \right), \quad r > 2M.$$

Eq. (2) can also be obtained for other spins. The corresponding Regge-Wheeler potential for spins $s = 0, 1, 2$ is given as [6]

$$V(r(r_*)) = \left(1 - \frac{2M}{r}\right) \left[\frac{l(l+1)}{r^2} + \frac{2M(1-s^2)}{r^3} \right] \quad (4)$$

where, $l \geq s$. Note that as we move from $r = r_0 = 2M$ at the event horizon to $r = \infty$, the tortoise coordinate varies from $-\infty$ to ∞ . Since the scattering problem with the radial coordinate r in three dimensions (3D) gets mapped into a one-dimensional (1D) one with the r_* coordinate, the Schrödinger-like equation (2) in black hole scattering can be solved using standard techniques for 1D tunneling in quantum mechanics. The asymptotic solutions of the Schrödinger equation (2) are

$$\psi(r_*) = A(\omega)e^{+i\omega r_*} + B(\omega)e^{-i\omega r_*}, \quad r_* \rightarrow -\infty,$$

$$\psi(r_*) = C(\omega)e^{+i\omega r_*} + D(\omega)e^{-i\omega r_*}, \quad r_* \rightarrow +\infty.$$

For waves incident on the black hole from the right (i.e. $+\infty$) we have $B(\omega) = 0$, the reflection amplitude $R(\omega) = D(\omega)/C(\omega)$ and the transmission amplitude $T(\omega) = A(\omega)/C(\omega)$, so that

$$\psi(r_*) = T(\omega)e^{i\omega r_*}, \quad r_* \rightarrow -\infty,$$

$$\psi(r_*) = e^{i\omega r_*} + R(\omega)e^{-i\omega r_*}, \quad r_* \rightarrow +\infty.$$

B. Critical parameters for black hole orbiting

An anomalous large angle scattering, called ALAS, was observed often in nuclear reactions between α -like nuclei such as ^{12}C - ^{16}O , ^{16}O - ^{28}Si etc [7] and has been attributed to the orbiting mechanism in scattering. The origin of this mechanism can be traced back to classical dynamics, where a particle approaching the potential center can get trapped in a circular orbit of radius r_0 if its energy equals the maximum of the effective potential at r_0 . Ford and Wheeler [2] found the connection of this phenomenon with the classical deflection function which becomes singular at a critical value of the angular momentum for which the circular orbit can exist and leads to divergent cross sections. The analogous effect in quantum mechanical scattering corresponds to the appearance of a diffraction pattern (or peaks) in the scattering cross section in the backward direction.

1. Deflection function in glory and orbiting

It was shown in [2] that as long as the classical deflection function $\Theta(l)$ remains between 0 and $\pm\pi$, the semi-classical cross section can be entirely described by the classical cross section. If the deflection function passes smoothly through 0 or $\pm\pi$, it leads to the phenomenon named glory. Though classically it corresponds to a singularity in the cross section, quantum mechanically one expects only a prominent peak in the cross section. Ford and Wheeler related the deflection function to the real part of the quantum mechanical scattering phase shift. Detailed discussions on the topic can be found in [2] and [8]. Here we directly state their conclusion, namely,

$$\Theta(l) = 2 \frac{d\delta_l^R}{dl} \quad (5)$$

connecting the deflection function with the real part of the phase shift. There exists a critical value l_g corresponding to backward glory scattering. The deflection function at backward angles can be approximated as

$$\Theta(l) = \pi + a(l - l_g). \quad (6)$$

Orbiting occurs when the effective potential as a function of the radial coordinate r possesses for some angular momentum l_C , a relative maximum equal to the available energy.

For massive particles in classical General Relativity (GR) this means $V_{eff}^{m \neq 0}(r_C, l_C) = E$. V_{eff} enters the geodesic equation in the form $\dot{r}^2/2 + V_{eff} = \text{const}$. For massless particles, the same condition with V_{eff} from the geodesic equation of motion is

$$\left(\frac{dV_{eff}(\ell_C)}{dr} \right)_{r_C} = 0, \quad V_{eff}(r_C, \ell_C) = \omega^2, \quad (7)$$

with

$$V_{eff}(r) = \frac{\ell^2}{2r^2} - \frac{M\ell^2}{r^3}. \quad (8)$$

where ℓ has the dimension of angular momentum per mass which makes V_{eff} dimensionless. Replacing ℓ^2 by $l(l+1)$ we return back to the quantum mechanical picture. Note that part of V (i.e. the first term of $V(r)$ in (4)) is proportional to V_{eff} and in the case of $s=1$, the entire $V(r)$ is proportional to V_{eff} . We shall come back to this point later. Under such a condition, the deflection function was shown to vary logarithmically

$$\begin{aligned} \Theta(l) &= \theta_1 + b \ln \left(\frac{l - l_C}{l_C} \right), \quad l > l_C, \\ \Theta(l) &= \theta_2 + 2b \ln \left(\frac{l_C - l}{l_C} \right), \quad 0 \leq l < l_C, \end{aligned} \quad (9)$$

where θ_1 , θ_2 and b are constants. The particle is expected to spiral below or above the barrier depending on the value of l being greater or less than l_C , respectively. If $l = l_C$, the particle is trapped in a circular orbit and $\Theta(l)$ is singular. With $\Theta(l)$ being related to the real phase shift as in (5), one expects a steep jump down in the real part of the phase shift at the critical value of l .

2. Radius of the unstable orbits and critical l

In black hole scattering with $s = 1$, Eq. (4) is proportional to the classical V_{eff} from General Relativity. Here one expects an unstable photon orbit at $r_C = 3M$. Considering the potential $V(3M) = \omega^2$ with the semi-classical prescription of $l(l+1) \rightarrow (l+1/2)^2$, it is easy to see that the critical value of the angular momentum l is given by $l_C = (3\sqrt{3}/2)\omega r_0 - 1/2$, where $r_0 = 2M$. If one uses $l_C(l_C + 1)$ instead, one of course ends up with a quadratic equation for l_C . The two values of l_C should however be quite close for large values of l . One could try to find the critical l_C for the occurrence of circular orbits in the scattering of spin 0 and 2 particles in the same way too. Considering $V(r)$ in (4) at $r = 3M$ leads to

$$l_C^{WKB} = \sqrt{\frac{27}{4}\omega^2 r_0^2 - \frac{2}{3}(1-s^2)} - \frac{1}{2}, \quad (10)$$

in the semi-classical approximation and

$$l_C^{QM} = \sqrt{\frac{27}{4}\omega^2 r_0^2 - \frac{2}{3}(1-s^2) + \frac{1}{4}} - \frac{1}{2} \quad (11)$$

quantum mechanically. In Table I we list the two sets of l_C for different values of ωr_0 . As expected, the difference between the semi-classical l_C^{WKB} and l_C^{QM} is little for large values of l . Note that for $s = 0$, there exists a critical ωr_0 below which one cannot find a real l_C .

Instead of taking the value of the potential at $r = 3M$ which corresponds to the maximum in the classical effective potential, we now find $V(r_C)$ (where r_C corresponds to the point where the maximum in $V(r)$ occurs) and use it to find the critical l_C . Thus, setting $dV/dr = 0$, we find

$$r_C = \frac{3r_0}{4} \left(1 - \frac{(1-s^2)}{L^2} \right) \left[1 \pm \sqrt{1 + \frac{32}{9} \frac{L^2(1-s^2)}{(L^2 - 1 + s^2)^2}} \right] \quad (12)$$

where, $L^2 = l_C(l_C + 1)$. Evaluating $V(r_C)$, one can now find l_C by looking for the zeros of the function $r_0^2 V(r_C) - \omega^2 r_0^2$. In Table II, we list the values of critical l_C evaluated as above for

TABLE I: Critical values of l obtained using $V(r = 3M)$. The numbers outside parentheses correspond to l_C^{WKB} and those inside to l_C^{QM} .

ωr_0	$s = 0$	$s = 1$	$s = 2$
0.5	-	0.799 (0.892)	1.4203 (1.484)
1	1.966 (2.017)	2.098 (2.145)	2.458 (2.5)
2	4.632 (4.656)	4.696 (4.720)	4.885 (4.908)
2.5	5.944 (5.963)	5.995 (6.014)	6.147 (6.166)
3	7.251 (7.267)	7.294 (7.310)	7.422(7.437)

TABLE II: Critical values of l obtained using $V(r = r_C)$

ωr_0	$s = 0$	$s = 1$	$s = 2$
0.5	0.618	0.892	1.497
1	2.016	2.145	2.504
2	4.656	4.720	4.909
2.5	5.963	6.014	6.167
3	7.267	7.310	7.438

the scattering of spin 0, 1 and 2 particles. The reader will notice that apart from the value of l_C which cannot be determined for $\omega r_0 = 0.5$ ($s = 0$) in Table I, the remaining values are quite close to those in Table II. What appears at a first glance as a curious coincidence will be explained in the next section by analyzing the form of $V(r)$.

In what follows, we shall present an exact numerical calculation of the reflection coefficient and study its behaviour as a function of l in context with orbiting scattering.

III. REFLECTION COEFFICIENT AND CHARACTERIZATION OF CIRCULAR ORBITS

In this section we will compare and discuss three different methods to calculate the reflection coefficient: a semi-analytical result, numerical results using the variable amplitude method and the approximation of a rectangular barrier adjusted to the problem of black hole scattering. We will see that the semi-analytical result gives a very good overall description

of the problem. The reflection amplitude in black hole scattering has also been calculated in literature [4] using semi-classical approximations.

A. Semi-analytical results

Before we go over to the details of the calculations of the reflection coefficient, let us briefly examine the nature of the potential in black hole scattering and what results one can expect. The potential in the Schwarzschild case as given in Eq.(4) is made up of two functions, namely, $U(r)$ (see Eq. (3)) and $f(r)$, such that $V(r) = f(r) U(r)$. $U(r)$ consists of a l dependent term which resembles the centrifugal barrier in standard problems in quantum mechanics. The form of $f(r)$ depends on the metric under consideration. In Fig. 1, we plot the potential as a function of the coordinate r as well as r_* and note the following features

- (i) The potential looks very different when taken as a function of r or r_* .
- (ii) If we plot the function $U(r)$ only, the steep rise of the centrifugal barrier is evident, however, only when plotted as a function of r and not r_* .
- (iii) Due to the presence of $f(r)$, the potential plotted as a function of r_* resembles a Gaussian barrier and the centrifugal term is not explicitly seen in the shape of the potential. However, as evident from Fig.2 the height of the potential rises with l .

New insights can be often gained by searching for analytical and semi-analytical results. To this end we notice that the reflection coefficients for the potential

$$U(x) = \frac{U_0}{\cosh^2(\alpha x)} \quad (13)$$

(or modification of the above by a shift of the argument) can be obtained analytically (we refer the reader for details to [9]). The relevance of this potential to our problem is its similarity to the Regge-Wheeler potential in the tortoise coordinate. Indeed,

$$r_0^2 V(r(r_*)) \approx \frac{r_0^2 V_0}{\cosh^2(r_*/ar_0 - b)} \quad (14)$$

fits the Regge-Wheeler potential quite well for $s = 0, 1, 2$ provided we choose $a = 2.4$, $b = 0.4$ and the height V_0 to be the Regge-Wheeler potential at $r = 3M$, i.e., $V_0 = V(r = 3M)$ which is different for different choices of s and l -dependent. For instance, in the cases $s = 0, 1, 2$

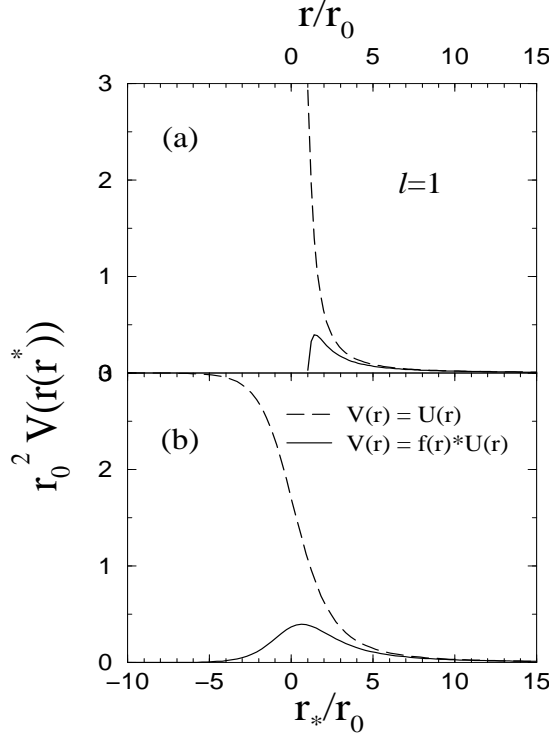


FIG. 1: The Schwarzschild black hole potential for spin $s = 0$ and $l = 1$. (a) Potential plotted as a function of the dimensionless coordinate r/r_0 and (b) r_*/r_0 , where r_* is the tortoise coordinate and r_0 the Schwarzschild radius.

we obtain

$$\begin{aligned}
 r_0^2 V_0 &= \frac{1}{27} \left[4l(l+1) + \frac{8}{3} \right], \quad s = 0 \\
 r_0^2 V_0 &= \frac{4}{27} 4l(l+1), \quad s = 1 \\
 r_0^2 V_0 &= \frac{1}{27} [4l(l+1) - 8], \quad s = 2
 \end{aligned} \tag{15}$$

The comparison between the Regge-Wheeler and the parametrized \cosh^{-2} potential is shown in Fig.2. Evidently, one would expect some quantitative agreement in both cases for the reflection coefficient for tunneling at higher energies, i.e., where the two potentials almost overlap. We will see that this is indeed the case. To be able to use the analytical results from [9] we use: $k^2 = \omega^2$, $\alpha = 1/ar_0$ and $2mU_0 = V_0$. This gives the following transmission coefficients:

$$|T_l|^2 = \frac{\sinh^2(a\pi\omega r_0)}{\sinh^2(a\pi\omega r_0) + \cos^2(\pi/2\sqrt{(1 - 4V_0 a^2 r_0^2)})} \tag{16}$$

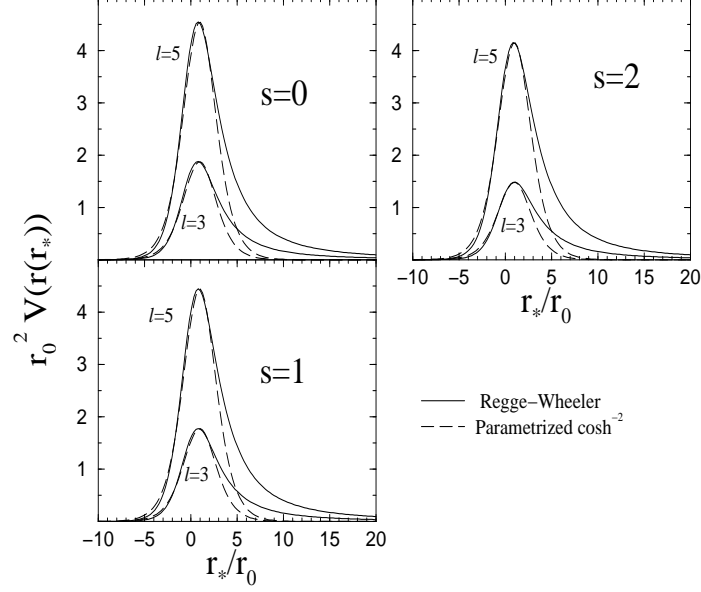


FIG. 2: The Regge-Wheeler potential compared with the \cosh^{-2} potential from equation (14) for different spins and angular momentum. The discrepancy between the two cases is more prominent at smaller energies where the Regge-Wheeler potential displays an asymmetric tail. Notice also that increasing l results in an increasing height.

if $4V_0a^2r_0^2 < 1$ and

$$|T_l|^2 = \frac{\sinh^2(a\pi\omega r_0)}{\sinh^2(a\pi\omega r_0) + \cosh^2(\pi/2\sqrt{(4V_0a^2r_0^2 - 1)})} \quad (17)$$

for $4V_0a^2r_0^2 > 1$. The Pöschl-Teller potential defined in equations (13) and (14) has been used to extract quasi-normal modes of black holes, either as an approximation [10] or in obtaining exact results in the Nariai spacetime [11] for which the scalar field equation reduces to the radial equation with the Pöschl-Teller potential.

B. The rectangular barrier approximation

In [1] Handler and Matzner used a rectangular barrier as an approximate solution to obtain the transmission coefficients corresponding to the black hole scattering problem of spin 1 particles. Their choice of the height of the barrier is V_0 with the same definition as explained above. The width b is energy and l dependent: $b = l/\omega$. The standard analytical

results for the rectangular barrier read for $(\omega r_0)^2 < r_0^2 V_0$

$$|T_l|^2 = \frac{1}{1 + \frac{r_0^4 V_0^2 \sinh^2(y)}{4[r_0^4 V_0 \omega^2 - \omega^4 r_0^4]}} \quad (18)$$

with $y \equiv l\sqrt{r_0^2 V_0 / \omega^2 r_0^2 - 1}$. For $r_0^2 V_0 < (\omega r_0)^2$ one obtains

$$|T_l|^2 = \frac{1}{1 + \frac{r_0^4 V_0^2 \sin^2(\tilde{y})}{4[\omega^4 r_0^4 - r_0^4 V_0 \omega^2]}} \quad (19)$$

with $\tilde{y} \equiv l\sqrt{1 - r_0^2 V_0 / \omega^2 r_0^2}$. Notice that with this prescription one cannot calculate T for $l = 0$ which as far as the results of Handler and Matzner are concerned is a valid assumption as they restrained themselves to $s = 1$ and therefore via $l \geq s$ to $l > 0$.

C. The variable amplitude method

In this section, $R_l(\omega)$ will be evaluated numerically via the variable amplitude method. The variable amplitude method was first introduced in [12] and has been widely used to evaluate the reflection and transmission coefficients for different potentials in literature [13]. This method involves writing the solution of the Schrödinger equation as a superposition of the reflected and transmitted waves, namely, $\psi_l(\omega, r_*) = T_l(\omega, r_*)[e^{i\omega r_*} + R_l(\omega, r_*)e^{-i\omega r_*}]$, which leads to the following equation for R_l

$$\frac{dR_l(\omega, r_*)}{dr_*} = -\frac{V(r_*)}{2i\omega} [e^{i\omega r_*} + R_l(\omega, r_*)e^{-i\omega r_*}]^2. \quad (20)$$

The absence of reflection behind the potential at $r_* \rightarrow -\infty$ imposes the boundary condition $R_l(\omega, -\infty) = 0$ on the above equation. The reflection coefficient is given by $|R_l|^2 = |R_l(\omega, \infty)|^2$.

D. Comparison of the methods and discussion of the results

When we calculate the reflection coefficient, we expect it to be large and close to unity for energies much below the height of the barrier (where transmission is a quantum mechanical possibility and hence very small). Since transmission increases with energy, the reflection coefficient falls and at high energies (above the barrier) where transmission becomes the classical phenomenon and reflection a quantum mechanical effect, the reflection coefficient is

negligibly small. In Fig. 3, we show the reflection coefficient as a function of energy for black hole scattering. On the left is shown the exact numerical result using the Regge-Wheeler potential and on the right the reflection coefficient evaluated from the expressions for $|R_l|^2 = 1 - |T_l|^2$ discussed in the previous sections for a rectangular barrier and parametrized \cosh^{-2} potential (which is similar in shape to a Gaussian barrier [14]). In Fig. 3 we have plotted

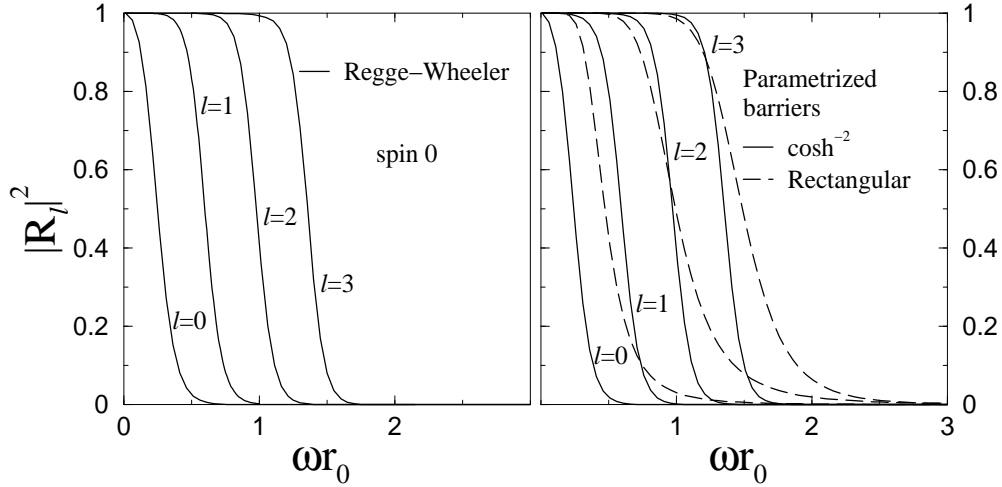


FIG. 3: Reflection coefficient as a function of energy for $s = 0$ and for different values of l in black hole scattering. On the left we plot the numerical results and on the right the reflection coefficient for an adjusted rectangular barrier (see text) of height V_0 (dashed line) and for the parametrized \cosh^{-2} potential (solid line). Since the results for the latter almost coincide with the numerical ones we plot them in two different boxes.

the results in two separate boxes since the numerical results would almost overlap with the results obtained from the \cosh^{-2} potential. This agreement is remarkable. In contrast to that, the results obtained via the rectangular potential differ from the exact (numerical) results.

In Fig. 4, we plot the numerically evaluated reflection coefficient as function of l for different values of ωr_0 and for different spins of the scattering particles. It is interesting to note that $|R_l|^2$ goes through a sudden rise at the critical values of l listed in the tables and connected to the orbiting phenomenon. The fact that the reflection coefficient for a given energy rises as a function of l can be understood by examining the plot of the potential for different l values at the same energy. In Fig. 2, we see that the effect of increasing l

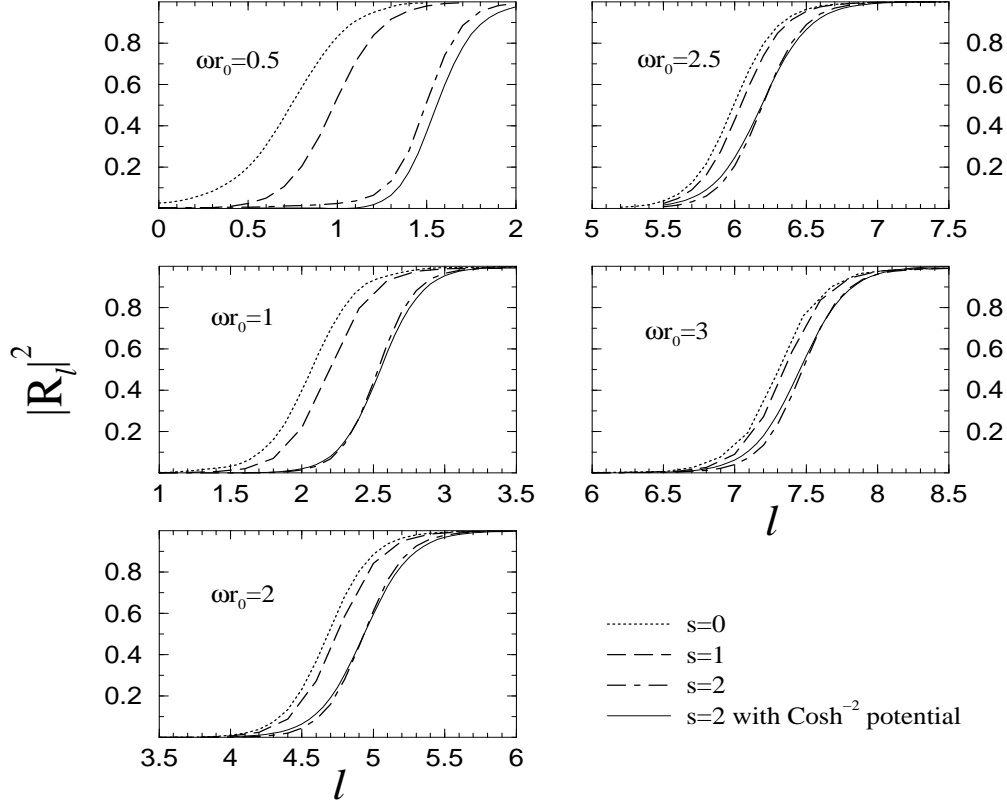


FIG. 4: Reflection coefficient or the scattering amplitude squared as a function of l for the scattering of massless scalar ($s = 0$), electromagnetic ($s = 1$) and gravitational ($s = 2$) waves from a black hole. For comparison we plot also for $s = 2$ the results obtained from the parametrized cosh^{-2} potential. As expected the agreement with numerical results improves with energy. For $s = 1$ the same comparison is done in the next figure. For $s = 0$, we just mention that here the agreement between the numerical and the semi-analytical results is the best among the three cases.

is to increase the height of the barrier. Hence, for example, an energy close to the top of the barrier for $l = 3$ will lead to little reflection but at the same energy, the barrier for $l = 7$ is much higher leading to larger reflection. For $s = 2$ we made a comparison with the corresponding cosh^{-2} potential. For small energies, the agreement is still not perfect, but improves rapidly with growing energies as is evident from the plots. This behaviour is to be expected since the Regge-Wheeler potential differs from the fitted cosh^{-2} case if the energy of the particle is much below the height of the potential where the Regge-Wheeler displays an asymmetric tail. This small mismatch between the the results obtained from the two potentials should be also present for the cases $s = 0, 1$, but will not be so prominent as for

$s = 2$. The reason is that $|R_l|^2$ for $s = 0, 1$ saturates at smaller value of l . As a result the difference between the small energy and the height is less then in the case $s = 2$ where the saturation sets in at higher l . Indeed, as one can infer from Fig. 5 the agreement between the exact results for the Regge-Wheeler and the \cosh^{-2} potential is remarkably good for $s = 1$ even for small energies.

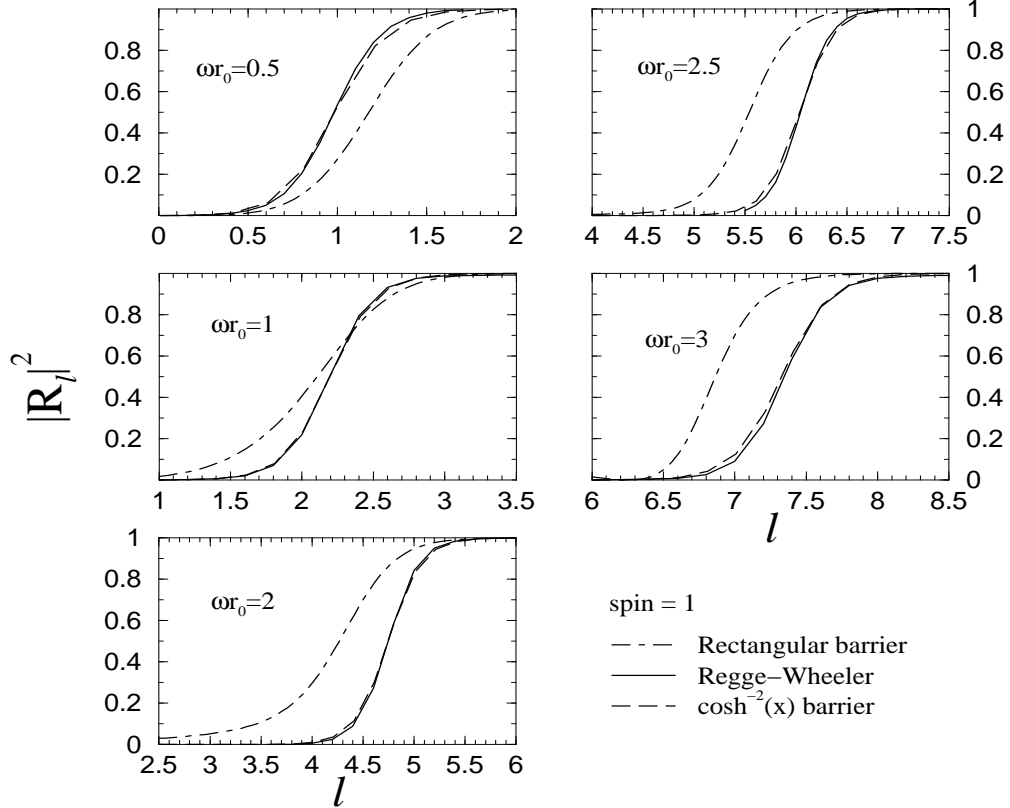


FIG. 5: Comparison of the reflection coefficients calculated using numerical methods, the adjusted rectangular barrier and the parametrized \cosh^{-2} potential as a function of l for the case $s = 1$. Evidently the rectangular barrier (dash-dotted) is not a good approximation whereas the \cosh^{-2} (dashed lines) gives a very good agreement with exact numerical results (solid lines).

An approximate calculation of the magnitude of the reflection amplitude was done in the third reference in [1] (article by Handler and Matzner). For the case of $s = 1$, the authors approximated the potential by a rectangular barrier as explained before in the text and studied the features of the corresponding reflection amplitude as a function of the angular momentum l . The magnitude of the reflection amplitude for the various values of ωr_0 studied here, started saturating to unity at a certain value of l which the authors referred to as l_g ,

the critical value for the onset of glory scattering. It also showed a sudden rise through $1/2$ as a function of l (this l value however is different for the rectangular and realistic Regge-Wheeler case). However, no interpretation was attempted to explain this fact. Indeed, here we have clearly connected it to the orbiting effects. The findings in [1] are not similar to those of the present work for the case $s = 1$. A closer look at Fig. 5 reveals the differences between the exact results and the results from a rectangular barrier. Not only is the shape of the reflection coefficients different, but also the values at which the reflection coefficient makes a jump and at which it saturates to unity.

A possible explanation for $|R_{l_C}|^2 = 1/2$ as seen in Figs 4 and 5 for the numerical results can be found by examining the approximate expression of the reflection coefficient as obtained in the WKB approximation [16]. In case of barrier penetration, when the energy ω^2 of the incident particle lies below the top of the barrier, the semi-classical reflection coefficient is given as

$$|R_l|^2 = \frac{\exp(2K_l)}{1 + \exp(2K_l)} \quad (21)$$

with

$$K_l = \int_{r_1}^{r_2} \sqrt{V(r_*) - \omega^2} dr_*,$$

where r_1 and r_2 are the classical turning points. For very small values of ω^2 , $|R_l|^2$ approaches unity. However, when ω^2 equals the maximum height of the barrier, $r_1 \simeq r_2$, $K \rightarrow 0$ and $|R_l|^2 \rightarrow 1/2$. Thus one can relate the orbiting phenomenon with a critical l value l_C such that $|R_{l_C}|^2 = 1/2$.

E. Imaginary scattering phase shift

Finally an interesting observation in connection with the orbiting is that the reflection coefficient which characterizes the critical value l_C is related to the imaginary part of the scattering phase shift. If one relates the reflection amplitude to the S matrix in three dimensional (3D) scattering, one can write $R_l(\omega) = \exp(2i\delta_l(\omega))$, where $\delta_l(\omega) = \delta_l^R(\omega) + i\delta_l^I(\omega)$ in general, is the complex scattering phase shift. Thus, $R_l(\omega) = \eta_l(\omega) \exp(2i\delta_l^R(\omega))$, where, $\eta_l(\omega) = \exp(-2\delta_l^I(\omega))$ is known as the inelasticity parameter which can be less than or equal to 1. In the 1-dimensional case, the S matrix is a 2×2 matrix with two channels, namely, transmission and reflection such that $|T|^2 + |R|^2 = 1$. If $\eta_l(\omega) = 1$, it implies that

$|R_l(\omega)|^2 = 1$ and there exists complete reflection. However, $\eta_l(\omega) = \exp(-2\delta_l^I(\omega)) < 1$ corresponds to the existence of the transmission channel. The reflection coefficient $|R_l|^2 = |\eta_l(\omega) \exp(2i\delta_l^R(\omega))|^2 = \eta_l^2(\omega)$, i.e., $|R_l(\omega)|^2 = \exp(-4\delta_l^I(\omega))$ and is related only to the imaginary part of the phase shift. The sudden rise in $|R_l(\omega)|^2$ at l_C corresponds to a peak in $d|R_l|^2/dl$, where

$$\frac{1}{|R_l|^2} \frac{d|R_l|^2}{dl} = -4 \frac{d\delta_l^I}{dl}. \quad (22)$$

This should be contrasted with the semi-classical characterization in Eq. (5) where the orbiting and glory parameters are characterized using the real part of the scattering phase shifts. This is also due to the fact that the scattering phase shifts calculated within the semi-classical approaches such as the WKB are always real. Using an exact numerical evaluation of $|R_l|^2$ here, we find a connection of the orbiting parameters with the imaginary part of the phase shift.

IV. RE-INTERPRETATION OF THE REGGE-WHEELER POTENTIAL

For $s = 1$ ($V_{eff} \propto V$), r_C obtained from (7) agrees with the quantum mechanical calculation via $(d^2|R_l|^2/dl^2)_{l=l_C} = 0$ (corresponding to the jump in $|R_l|^2$). The same would be true for $s = 0, 2$ if r_C is computed through Eq.(7), replacing therein V_{eff} by V . The argument for $s = 0, 2$, namely, that l_C is connected to the classical unstable circular orbit, can be now maintained if we attempt a reinterpretation of V . Restoring \hbar in our expressions amounts to replacing $e^{i\omega t}$ by $e^{i(E/\hbar)t}$ or equivalently ω by E/\hbar . The Schrödinger-like equation then reads

$$\left[-\hbar^2 \frac{d^2}{dr_*^2} + \hbar^2 V(r) \right] \psi_{nl\omega} = E^2 \psi_{nl\omega}. \quad (23)$$

Identifying $\hbar^2 l(l+1)$ with L^2 , we can write

$$\begin{aligned} \hbar^2 V &= 2 \left[\tilde{V}_{eff} + \hbar^2 \frac{M(1-s^2)}{r^3} \left(1 - \frac{2M}{r} \right) \right], \\ \tilde{V}_{eff} &= \left(1 - \frac{2M}{r} \right) \frac{L^2}{r^2}. \end{aligned} \quad (24)$$

In identifying $\hbar^2 l(l+1)$ by L^2 , we are going back from quantum mechanics to classical physics. It is reasonable to speculate that $\hbar^2 V$ represents the full effective potential, i.e., the classical part plus \hbar^2 quantum mechanical corrections. Indeed, $\hbar^2 V$ would then be the correct tool to calculate a classical unstable orbit. Recently, \hbar corrections to the Newtonian

potential, have been discussed in [15], where it was found that the additional terms are proportional to $\hbar M_1 M_2 G^2 / r^3$ (G is the restored Newtonian constant). The procedure to arrive at such a result is to consider non-relativistic amplitudes with zero and higher order loop corrections. The difference from our case is that these corrections were calculated for massive particles where the Newtonian potential exists and the non-relativistic limit makes sense. In a massless case, such a procedure is not well-defined. Therefore our conjecture is well motivated but remains open. Since the dimensions of V_{eff} from GR and \tilde{V}_{eff} are different, let us be more specific. To make $\hbar^2 V$ dimensionless we divide it by the Planck mass squared, E_{Pl}^2 and identify $L^2 / E_{Pl}^2 = \ell^2$. Thus,

$$\frac{\hbar^2 V}{E_{Pl}^2} = 2 \left[V_{eff} + \hbar \frac{2G^2 M(1-s^2)}{r^3} \left(1 - \frac{2GM}{r} \right) \right]. \quad (25)$$

Our speculation is simply to say that V_{eff} receives a small quantum correction proportional to \hbar in the above equation. This explains also the coincidences found in the previous section. Indeed, calculating r_C from V_{eff} or V_{eff} plus quantum corrections will give very similar results. Therefore it is not a surprise that l_C^{QM} comes out quite close to the l_C evaluated from r_C .

V. SUMMARY

The behaviour of the reflection coefficient, $|R_l|^2$, which enters the scattering cross sections is investigated for the scattering of scalar, electromagnetic and gravitational waves from a Schwarzschild black hole. We paid special attention to the issue of orbiting effects in a quantum mechanical scattering off black holes. Our investigation displays the following features:

1. For $s = 0, 1, 2$ we found that $|R_l|^2$ jumps at a certain critical value l_C , i.e. its second derivative with respect to l is zero. The Regge-Wheeler potential is proportional to the classical effective potential for $s = 1$ only. We find that l_C is connected with the unstable circular orbit at $r_C = 3M$ for $s = 1$.
2. We find the l_C values for $s = 0, 2$, too. Here also we would expect that the critical value l_C is connected to an unstable circular orbit at a critical r_C . Interestingly, the l_C values calculated using $V(r_C)$ lie very close to those using $V(3M)$. This can be explained if

we re-interpret the Regge Wheeler potential as the classical effective potential with \hbar corrections. Notice that with the values of l_C obtained via the rectangular potential, such a conclusion would be impossible as the jump occurs at a different l_C and the connection to the unstable circular orbit is lost.

3. For all values of ωr_0 and spins 0, 1 and 2 we find that $|R_{l_C}|^2 = 1/2$.
4. We have shown that the transmission and reflection coefficients of the potential proportional to $\cosh^{-2}(\alpha x - \beta)$ (Pöschl-Teller) match very well with the exact results. Since for this particular case the transmission coefficient can be given analytically, this allows us to study the black hole scattering in a semi-analytical way and supplements the conclusion that such a potential is a good approximate tool in black hole physics [10, 11]. Both the semi-analytical results and the numerical ones refine approximate results obtained elsewhere and reveal some deficiencies of the approximation methods.

-
- [1] L. C. B. Crispino, S. R. Dolan and E. S. Oliveira, Phys. Rev. Lett. 102, 231103 (2009); S. R. Dolan, E. S. Oliveira and L. C. B. Crispino, Phys. Rev. D. 79, 064014 (2009); F. A. Handler and R. A. Matzner, Phys. Rev. D **22**, 2331 (1980); R. A. Matzner, C. DeWitt Morette, B. Nelson and T-R Zhang, Phys. Rev. D **31**, 1869 (1985); P. Anninos *et al.*, Phys. Rev. D **46**, 4477 (1992); S. R. Dolan, Phys. Rev. D **77**, 044004 (2008).
 - [2] K. W. Ford and J. A. Wheeler, Ann. Phys. **7**, 259 (1959); *ibid*, **7**, 287 (1959).
 - [3] N. F. Mott and H. S. W. Massey, *The Theory of Atomic Collisions*, second edition, Clarendon Press, Oxford (1949).
 - [4] R. Fabbri, Phys. Rev. D **12**, 933 (1975).
 - [5] N. Sanchez, Phys. Rev. D **18**, 1030 (1978); *ibid*, Phys. Rev D **18**, 1798 (1978); J. A. H. Futterman, F. A. Handler and R. A. Matzner, *Scattering from Black Holes*, Cambridge University Press (1988); N. Anderson and B. Jensen, *Scattering by Black Holes in Scattering: scattering and inverse scattering in pure and applied science*, Academic Press (2002).
 - [6] J. Skakala and M. Visser, JHEP **1008**, 061 (2010).
 - [7] P. Braun-Munzinger and J. Barrette, Phys. Rep. **87**, 209 (1982).
 - [8] H. M. Nussenzveig, J. Math. Phys. **10**, 82 (1969); *ibid*, **10**, 125 (1969).

- [9] L. D. Landau and E. M. Lifshitz, “Quantum Mechanics (Non-relativistic Theory)”, Course of Theoretical Physics, Volume 3, Third edition, Butterworth-Heinemann 1991
- [10] V. Ferrari and B. Mashhoon, Phys. Rev. Lett. **52**, 1361 (1984).
- [11] V. Cardoso and J. P. S. Lemos, Phys. Rev. **D67**, 084020 (2003); S. Zerbini and L. Vanzo, Phys. Rev. **D70**, 04403 (2004).
- [12] Y. Tikochinsky, Ann. Phys. **103**, 185 (1977).
- [13] M. G. Rozman, P. Reineker and R. Tehver, Phys. Rev. A **49**, 3310 (1994); O. Kidun, N. Fominykh and J. Berakdar, Phys. Rev. A **71**, 022703 (2005); H. Lee and Y. J. Lee, J. Phys. A **40**, 3569 (2007).
- [14] F. M. Fernández, Am. J. Phys. **79**, 752 (2011).
- [15] J. F. Donoghue, Phys. Rev. Lett. **72**, 2996 (1994); N. E. J. Bjerrum-Bohr, J. F. Donoghue and B. R. Holstein, Phys. Rev. D **67**, 084033 (2003); H. W. Hamber and S. Liu, Phys. Lett. B **357**, 51 (1995); S. Bellucci and A. Shiekh, Phys. Lett. B **395**, 16 (1997); I. B. Kriplovich and G. G. Kirilin, J. Exp. Theor. Phys. **95**, 981 (2002); A. Ross and B. R. Ross, J. Phys. A: Math. Theor. **40** (2007) 6973.
- [16] N. Froeman and P. O. Froeman, *JWKB Approximation: Contributions to the Theory*, North-Holland, Amsterdam (1965).